Influence of Defects on the Luminescence Quantum Yield of $Y_{1.94}Eu_{0.06}O_3$

W. van Schaik* and G. Blasse

Debye Research Institute, University of Utrecht, P.O. Box 80000, 3508 TA Utrecht, The Netherlands

Received October 8, 1991. Revised Manuscript Received December 3, 1991

The influence of defects on the luminescence quantum yield of $Y_{1.94}Eu_{0.06}O_3$ is reported. A decrease of the quantum yield for 254-nm excitation is due to competitive absorption by defects. The presence of interstitial oxygen also leads to competitive absorption and hence to a decrease of the quantum yield for 254-nm excitation. Upon host lattice excitation energy transfer to interstitial oxygen competes with energy transfer to the Eu^{3+} ions and decreases the quantum yield for 185-nm excitation. Codoping with transition-metal ions results in strong competitive absorption and hence in a strong decrease of the quantum yield. Codoping with Tb and Ce leads to a decrease of the quantum yield due to competitive absorption by the tetravalent state of these ions.

Introduction

In 1974 Verstegen et al.[1] introduced the high-quality tricolor fluorescent lamp, based on rare-earth-metal phosphors. The unsurpassed red-emitting component is $Y_{1.94}Eu_{0.06}O_3$. This phosphor has a sharp emission line at 612 nm in which the larger part of the intensity is concentrated. Since the charge-transfer transition of Eu^{3+} has a good overlap with the most intense mercury discharge line (254 nm), direct excitation is possible.[2]

Research concerning the luminescence properties of Y_2O_3:Eu^{3+} has been extensive, since this is a commercial phosphor and a simple system.[3-8] However, as far as we are aware, only one study on the influence of impurities on the quantum yield of $Y_{1.94}Eu_{0.06}O_3$ has been published.[9] Since $Y_{1.94}Eu_{0.06}O_3$ is the most expensive component of the phosphor blend, it seems useful to determine the influence of defects on the quantum yield. The decrease of the quantum efficiency resulting from codoping with an impurity will be discussed using a competitive absorption mechanism.

First, the influence of lattice defects on the quantum yield of $Y_{1.94}Eu_{0.06}O_3$ is discussed. The lattice defects are introduced by codoping with cations with a different charge from Y^{3+} (Ca^{2+}, Zr^{4+}) and by changing the firing atmosphere. Subsequently the influence of transition-metal ions on the quantum yield has been studied. As colored ions we have also studied as examples Mn, Fe, and Cr. The starting materials for the phosphor preparation will also be contaminated by other rare-earth ions. It is expected that the rare-earth ions with different valencies exhibit the largest influence on the quantum yield. As good examples $Tb^{3+/4+}$ and $Ce^{3+/4+}$ have been studied.

The cubic bixbyite structure of C-Y_2O_3 is well-known.[10,11] Each rare-earth ion is surrounded by oxygens located at the corners of a cube. Two corners of the cube are not occupied by oxygen ions. The vacancies are either along a body diagonal or along a face diagonal of the cube. This results in S_6 and C_2 site symmetry, respectively (Figure 1). The interstitial sites are ordered as nonintersecting strings through the anion lattice and provide an easy pathway for interstitial oxygen diffusion.[12]

Experimental Section

Preparation. The measurements were performed on powder samples of composition $Y_{1.94}Eu_{0.06}O_3$:X (mol %). The impurity (X) concentration is between 0 and 1 mol %. The starting materials for all samples were Eu_2O_3 (Highways Int., 99.99%) and Y_2O_3 (Rhône-Poulenc, 99.99%). According to mass absorption spectrometry analysis, all other rare-earth ions are present in concentrations lower than 2 ppm. The transition-metal ions are present in concentrations lower than 2 ppm according to ICP analysis (Fe, Cr, Co, Ni, and Ti) and AAS analysis (Cu and Pb). The CaO content is also lower than 2 ppm.

The samples containing Zr^{4+}, Ca^{2+}, and the transition-metal ions were prepared by solid-state reaction. The starting materials were, after milling, fired in air (unless otherwise stated) at 1450 °C for 8 h.

The samples codoped with Tb or Ce were prepared by dissolving the rare-earth oxides in dilute nitric acid. Subsequently, the mixed oxalates were coprecipitated by adding a solution of oxalic acid (1.4 M). After washing and drying, the precipitate was fired in air at 1000 °C for 4 h. Blank $Y_{1.94}Eu_{0.06}O_3$ samples were made in both ways.

The crystal structure of all samples was checked by X-ray powder diffraction using Cu Kα radiation. Samples are single phase.

Optical Measurements. Diffuse reflection spectra were recorded on a Perkin-Elmer Lambda 7 UV–vis spectrophotometer using $BaSO_4$ as a reference. The excitation spectra from 300 to 190 nm were recorded on a Perkin-Elmer MPF-3L spectrofluorometer equipped with a water-cooled Hamamatsu 200-W deuterium lamp. The other spectra were recorded either on a Spex Fluorolog-2 spectrofluorometer or on a Perkin-Elmer MPF-44B spectrofluorometer, both equipped with an Oxford flow cryostat for measurements at liquid helium temperatures and with a xenon lamp as excitation radiation source. The excitation spectra were corrected for the lamp output. The emission spectra were corrected for the photomultiplier sensitivity.

The quantum yield was measured for 254-nm excitation and in some cases for 185-nm excitation (unless otherwise stated in the text, quantum yields are for 254-nm excitation). The quantum yield was measured by integrating the total emission intensity and dividing this by the absolute absorption at 254 or 185 nm, respectively. The quantum yields of the $Y_{1.94}Eu_{0.06}O_3$:X samples (X: impurity) are given relative to the quantum yield of a standard commercial $Y_{1.94}Eu_{0.06}O_3$ phosphor. It should be noted that our

(1) Verstegen, J. M. P. J.; Radielovic, D.; Vrenken, L. E. *J. Electrochem. Soc.* **1974**, *121*, 1627.
(2) Smets, B. M. J. *Mater. Chem. Phys.* **1987**, *16*, 283.
(3) Kotera, Y.; Higashi, T.; Sugai, M.; Ueno, A. *J. Lumin.* **1984**, *31, 32*, 709.
(4) Hunt, Jr., R. B.; Pappalardo, R. G. *J. Lumin.* **1985**, *34*, 133.
(5) Pappalardo, R. G.; Hunt, Jr., R. B. *J. Electrochem. Soc.* **1985**, *132*, 721.
(6) Buijs, M.; Meijerink, A.; Blasse, G. *J. Lumin.* **1987**, *37*, 9.
(7) Hintzen, H. T.; van Noort, H. M. *J. Phys. Chem. Solids* **1988**, *49*, 873.
(8) Klaasen, D. B. M.; van Ham, R. A. M.; van Rijn, T. G. M. *J. Lumin.* **1989**, *43*, 261.
(9) Fuller, M. J. *J. Electrochem. Soc.* **1981**, *128*, 1381.
(10) O'Connor, B. H.; Valentine, T. M. *Acta Crystallogr.* **1969**, *B25*, 2140.
(11) Faucher, M.; Pannetier, J. *Acta Crystallogr.* **1980**, *B36*, 3209.
(12) Norby, T.; Kofstad, P. *J. Am. Ceram. Soc.* **1984**, *67*, 786.

0897-4756/92/2804-0410$03.00/0

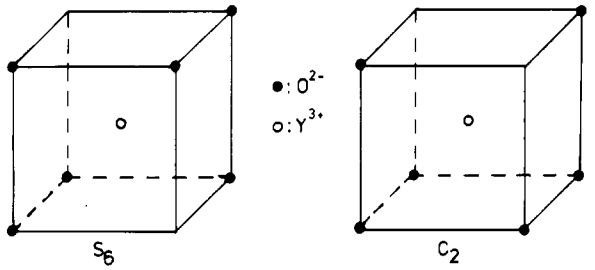

Figure 1. Oxygen surroundings of Y^{3+} in Y_2O_3.

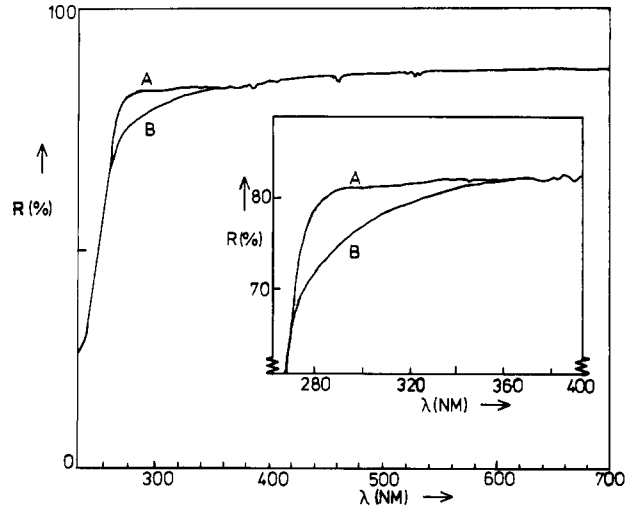

Figure 2. Reflection spectra of $Y_{1.94}Eu_{0.06}O_3:Ca^{2+}$ (A) and of $Y_{1.94}Eu_{0.06}O_3:Zr^{4+}$ (B). The inset shows an enlargement in the region where spectra A and B are different.

quantum yield values are not the quantum yield values of the Eu^{3+} ion itself but an overal quantum yield of the sample including codoped impurities.

Results and Discussion

Lattice Defects. We start with the results for Ca^{2+} and Zr^{4+} as impurities. Charge-compensating defects are necessary to preserve the electroneutrality, if Zr^{4+} is built into the Y_2O_3 lattice. Bratton[13] concluded that the extra net charge of Zr^{4+} is compensated for by doubly ionized oxygen interstitials. The interstitial oxygens fit well on the vacant sites of the anion lattice (Figure 1).

In Figure 2 we present the diffuse reflection spectra of $Y_{1.94}Eu_{0.06}O_3$ samples codoped with either Zr^{4+} (1 mol %) or Ca^{2+} (1 mol %). The very strong absorption band situated at wavelengths shorter than 280 nm is due to the charge-transfer transition of Eu^{3+}. The diffuse reflection spectrum of $Y_{1.94}Eu_{0.06}O_3:Zr^{4+}$ also shows a decrease of the reflection between 350 and 280 nm. This absorption is not caused by Eu^{3+} or Zr^{4+} and is ascribed to interstitial oxygen.

The quantum yield values for 254-nm excitation of our blank $Y_{1.94}Eu_{0.06}O_3$ samples and of $Y_{1.94}Eu_{0.06}O_3$ codoped with either Zr^{4+} or Ca^{2+} are given in Table I. The quantum yield is defined as the ratio between the number of emitted photons and the number of absorbed photons. If, besides the Eu^{3+} ion, defects absorb part of the excitation radiation and these defects exhibit no emission, the quantum yield will be decreased. Henceforth this process will be called competitive absorption.

The absorption due to the interstitial oxygen in $Y_{1.94}Eu_{0.06}O_3:Zr^{4+}$ will continue beyond 280 nm toward shorter wavelengths. Due to this competitive absorption

(13) Bratton, R. J. *J. Am. Ceram. Soc.* **1969**, *52*, 213.

Table I. Relative Luminescence Quantum Yield of $Y_{1.94}Eu_{0.06}O_3$:X at 300 K for 254-nm Excitation (Solid-State Reaction)

$Y_{1.94}Eu_{0.06}O_3$:X (X: impurity)	quantum yield
blank fired in air	84
blank fired in O_2	68
blank fired in N_2	96
1% Zr^{4+}	72
1% Ca^{2+}	99
1000 ppm Cr	45
1000 ppm Fe	30
1000 ppm Mn	8

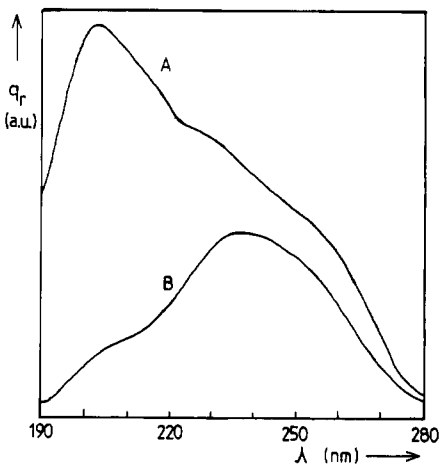

Figure 3. Room-temperature excitation spectra of the emission of Eu^{3+} (λ_{em} = 612 nm) in $Y_{1.94}Eu_{0.06}O_3:Ca^{2+}$ (A) and in $Y_{1.94}Eu_{0.06}O_3:Zr^{4+}$ (B). q_r gives the relative quantum output.

the quantum yield of $Y_{1.94}Eu_{0.06}O_3:Zr^{4+}$ is rather low.

Reabsorption of the Eu^{3+} emission or nonradiative energy transfer from Eu^{3+} to interstitial oxygens will not play a role, because there is no optical absorption due to the interstitial oxygens at the energy of the $^5D_0 \rightarrow {}^7F_J$ emission of Eu^{3+}.

Codoping with Ca^{2+} leads to a reduction of the concentration of interstitial oxygens.[14] The diffuse reflection spectrum (Figure 2) confirms the reduction of the number of interstitial oxygens, since the absorption band ascribed to these defects is absent. The absence of competitive absorption results in a higher quantum yield for 254-nm excitation of $Y_{1.94}Eu_{0.06}O_3:Ca^{2+}$ compared to the sample codoped with Zr^{4+} (Table I).

The concentration of interstitial oxygens depends on the oxygen pressure applied during the firing procedure. In the reflection spectrum of a blank $Y_{1.94}Eu_{0.06}O_3$ sample fired in N_2 the absorption band ascribed to interstitial oxygen is absent. The absence of competitive absorption in a sample fired in N_2 results in a similar high quantum yield as the sample codoped with Ca^{2+}.

The reflection spectra of the blank $Y_{1.94}Eu_{0.06}O_3$ samples fired in air or in O_2 show the same absorption band due to interstitial oxygen as $Y_{1.94}Eu_{0.06}O_3$ codoped with Zr^{4+}. In air, oxygen migrates into the yttria to create interstitial oxygen compensated for by electron holes.[12,15,16] The quantum yield values of the blank samples fired in air or O_2 are rather low due to the competitive absorption by the interstitial oxygen.

In Figure 3 the UV excitation spectra of the emission of Eu^{3+} (λ_{em} = 612 nm) in $Y_{1.94}Eu_{0.06}O_3:Ca^{2+}$ and in

(14) Katayama, K.; Ōsawa, H.; Akiba, T.; Urabe, K.; Yanagida, H. *J. Mater. Sci.* **1990**, *25*, 1503.
(15) Norby, T.; Kofstad, P. *J. Am. Ceram. Soc.* **1986**, *69*, 784.
(16) Hartmanová, M.; Morháčová, E.; Travenec, I.; Urusovskaya, A. A.; Knab, G. G.; Korobkov, I. I. *Solid State Ionics* **1989**, *36*, 137.

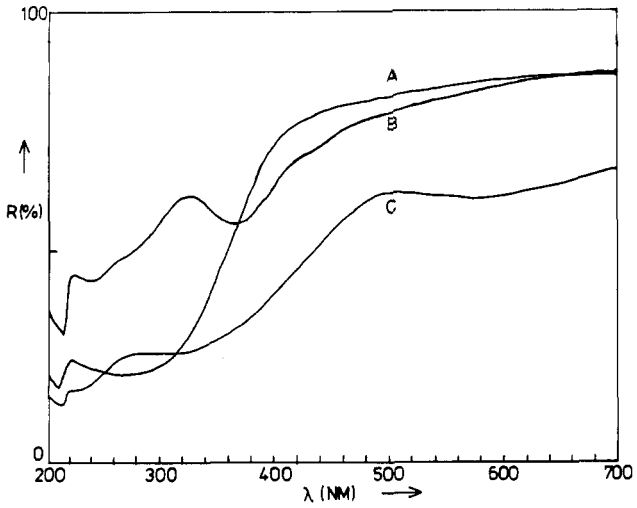

Figure 4. Reflection spectra of Y_2O_3:Fe (A), Y_2O_3:Cr (B), and Y_2O_3:Mn (C).

Table II. Relative Luminescence Quantum Yield of $Y_{1.94}Eu_{0.06}O_3$:X at 300 K for 185-nm Excitation (Solid-State Reaction)

$Y_{1.94}Eu_{0.06}O_3$:X (X: impurity)	quantum yield
blank fired in air	69
blank fired in N_2	89
1% Zr^{4+}	9
1% Ca^{2+}	86

$Y_{1.94}Eu_{0.06}O_3$:Zr^{4+} at room temperature are depicted. The excitation band at 235 nm is ascribed to the Eu^{3+}–O^{2-} charge-transfer transition. At wavelengths shorter than 220 nm the host lattice itself is excited[17,18] (Figure 4). The emission of pure yttria[18-21] for excitation at 200 nm consists of a structureless band at 360 nm at 4.2 K. This emission band is ascribed to the recombination of self-trapped excitons.

At room temperature the excitons are mobile. The energy is efficiently transferred to impurities.[18,22] Actually, in the emission spectrum at room temperature of our pure yttria (99.99%) there are for excitation at 200 nm, besides the intrinsic emission band, also emission lines due to Tb^{3+} and Dy^{3+}, although these ions are present in concentrations lower than 2 ppm. This shows how efficient the energy transfer is. The samples doped with 3 mol % Eu^{3+} show only Eu^{3+} emission and no intrinsic host lattice emission at room temperature.

The excitation band due to host lattice excitation is markedly less intense for Eu^{3+} in $Y_{1.94}Eu_{0.06}O_3$:Zr^{4+} than for Eu^{3+} in $Y_{1.94}Eu_{0.06}O_3$:Ca^{2+}. In the sample codoped with Ca^{2+} the energy transfer from the host lattice to the Eu^{3+} ions is obviously more efficient than in the sample codoped with Zr^{4+} (Figure 3). The interstitial oxygen ions, present as compensation for the tetravalent Zr^{4+} ions, are competing with the Eu^{3+} ions for the excitation energy. The self-trapped exciton emission overlaps the absorption band of the interstitial oxygen ions as required for energy transfer.

This leads to a low quantum yield of $Y_{1.94}Eu_{0.06}O_3$:Zr^{4+} for 185-nm excitation (Table II), whereas $Y_{1.94}Eu_{0.06}O_3$:Ca^{2+} has a high quantum yield for 185-nm excitation (Table II). This is in agreement with the intense host lattice excitation band of the Eu^{3+} emission in $Y_{1.94}Eu_{0.06}O_3$:Ca^{2+}.

The excitation spectrum of the emission of Eu^{3+} in the $Y_{1.94}Eu_{0.06}O_3$ sample which is fired in a N_2 atmosphere is similar to that of the sample codoped with Ca^{2+}. The excitation spectra of the samples fired in air and in O_2 and samples codoped with Zr^{4+} are also similar to each other. This is in accordance with the absence and presence of interstitial oxygen ions, respectively. This clearly shows that the trapping of the excitons is caused not by the Zr^{4+} ion itself but by the interstitial oxygens. The difference in quantum yield for 185-nm excitation between $Y_{1.94}Eu_{0.06}O_3$ fired in air and in N_2 is less pronounced than between samples codoped with either Zr^{4+} or Ca^{2+} (Table II).

Summarizing, the results on the influence of Ca^{2+} and Zr^{4+} doping, on the influence of the firing atmosphere, and on the ultraviolet excitation spectra can all be explained with one model based on interstitial oxygen.

Transition-Metal Ions. The influence of Fe, Mn, and Cr ions on the quantum yield of $Y_{1.94}Eu_{0.06}O_3$:X (X (1000 ppm) is Fe, Mn, or Cr) has been investigated. In Figure 4 the diffuse reflection spectra of Y_2O_3 doped with Fe, Mn, or Cr are shown.

The reflection spectrum of Y_2O_3:Fe shows one strong absorption band in the UV region of the spectrum. This band is ascribed to a charge-transfer transition of the trivalent Fe^{3+} ion.[23] It cannot be ascribed to a d–d transition in view of its high intensity and its broadness. Since Fe^{3+} is a d^5 ion, no d–d absorption features are to be expected in the reflection spectrum, since all the d–d transitions are parity and spin forbidden.[24,25]

Upon excitation in the charge-transfer band, the iron-containing sample does not luminesce, not even at 4.2 K. The luminescence may be either quenched by radiationless processes or situated too far in the infrared to be detected by the photomultiplier used. It should be noted that the Fe^{3+} ion replaces a host lattice cation which has a larger ionic radius than the Fe^{3+} ion itself.[26]

The reflection spectrum of Y_2O_3:Mn shows also a strong absorption band in the UV. Considering the absorption strength, this band is ascribed to a charge-transfer transition of Mn^{3+}. The weaker absorption band at about 575 nm is then ascribed to the only spin-allowed d–d transition of $Mn^{3+}(d^4)$ $^5E \rightarrow {}^5T_2$. At 4.2 K the Mn^{3+} ion in Y_2O_3 does not luminesce for charge-transfer excitation.

The absorption bands in the diffuse reflection spectrum of Y_2O_3:Cr cannot be assigned to transitions of trivalent Cr^{3+}. However, the diffuse reflection spectrum is rather similar to that of $CaCrO_4$ and K_2CrO_4 as given by Dalhoeven and Blasse.[27] Following the authors assignment of the chromate absorption bands, the shoulder at ~450 nm is ascribed to the $^1A_1 \rightarrow {}^1T_1$ ($t_1 \rightarrow 2e$) transition, the broad band at 380 nm to the $^1A_1 \rightarrow {}^1T_2$ ($t_1 \rightarrow 2e$) transition, and the absorption band at 260 nm to the $^1A_1 \rightarrow {}^1T_1$ ($4t_2 \rightarrow 2e$) transition. There appears to be a broad UV absorption band which is superimposed on the Cr^{6+} absorption bands. This band is ascribed to interstitial oxygen.

(17) Tomiki, T.; Tamashiro, J.; Tanahara, Y.; Yamada, A.; Fukutani, H.; Miyahara, T.; Kato, H.; Shin, S.; Ishigame, M. *J. Phys. Soc. Jpn.* **1986**, *55*, 4543.
(18) Kuznetsov, A. I.; Abromov, V. N.; Rooze, N. S.; Savikhina, T. I. *JETP Lett.* **1978**, *28*, 602.
(19) Toma, S. Z.; Palumbo, D. T. *J. Electrochem. Soc.* **1970**, *117*, 236.
(20) Hayes, W.; Kane, M. J.; Salminen, O.; Kuznetsov, A. I. *J. Phys. C: Solid State Phys.* **1984**, *17*, L383.
(21) Blasse, G.; Brixner, L. H. *Eur. J. Solid State Inorg. Chem.* **1991**, *28*, 767.
(22) Ratinen, H. *Acta Polytech. Scand.* **1971**, *107*, 2.
(23) Oomen, E. W. J. L.; van der Vlist, K.; Smit, W. M. A.; Blasse, G. *Chem. Phys. Lett.* **1986**, *129*, 9.
(24) Lever, A. B. F. *Inorganic Electronic Spectroscopy*, 2nd ed.; Elsevier: Amsterdam, 1984.
(25) Sugano, S.; Tanabe, Y.; Kamimura, H. *Multiplets of Transition Metals in Crystals*; Academic Press: New York, 1970.
(26) Shannon, R. D. *Acta Crystallogr.* **1976**, *A32*, 751.
(27) Dalhoeven, G. A. M.; Blasse, G. *Chem. Phys. Lett.* **1980**, *76*, 27.

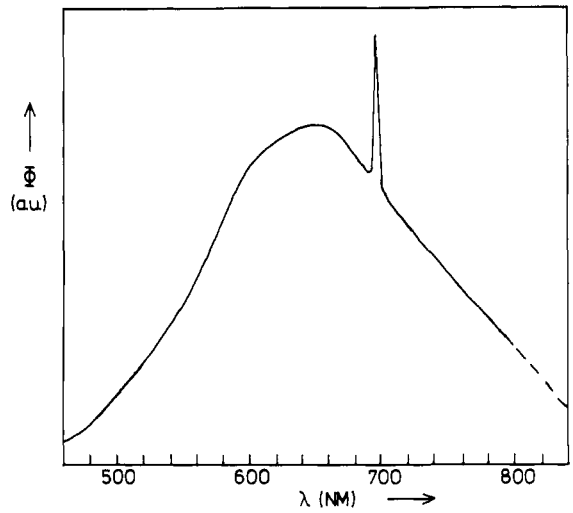

Figure 5. Emission spectrum of $Y_2O_3:Cr^{6+}$ at 4.2 K for excitation at 380 nm. Φ gives the radiant power per constant wavelength interval in arbitrary units.

The absorption band at 215 nm which is present in all three spectra (Figure 4) is caused by host lattice absorption.

The emission of the Cr-doped yttria at 4.2 K for 380-nm excitation consists of a broad structureless band with a maximum at 660 nm (Figure 5). This is in good agreement with the luminescence properties reported earlier[27] for CrO_4^{2-}. The emission intensity is very low. It was not possible to obtain an excitation spectrum of the emission band at 660 nm. No emission is observed for 280-nm excitation.

Huber et al.[28] observed the spin-allowed $^4T_2 \rightarrow {}^4A_2$ emission transition of Cr^{3+} in Sc_2O_3. The fact that we observed only Cr^{6+} and no Cr^{3+} in Y_2O_3 is rather surprising. The fact that we obtained another oxidation state than Huber et al. is probably due to the different synthesis procedure.

Despite the very small radius of the Cr^{6+} ion,[26] the Y_2O_3 lattice seems to be able to incorporate Cr^{6+}. The extra net positive charge of Cr^{6+} on a Y^{3+} site must be compensated for by interstitial oxygens. The presence of the interstitial oxygens makes it possible to create a tetrahedral coordination for the Cr^{6+} without deforming the lattice too much. However, it cannot be ruled out that the Cr^{6+} is present as a chromate phase on the surface of the yttria particles, as has been reported for chromate on silica.[29]

Besides the broad emission band at 660 nm, excitation at 380 nm at 4.2 K yields also a sharp emission line at 694 nm (Figure 5). This emission is ascribed to the $^2E \rightarrow {}^4A_2$ transition of Cr^{3+}. The occurrence of this spin-forbidden transition is characteristic of Cr^{3+} on an octahedral site with a strong crystal field.[30] Since in yttria the Cr^{3+} ion is expected to experience a small crystal field (as in $Sc_2O_3:Cr^{3+}$ (ref 28)), this sharp emission line cannot be caused by Cr^{3+} in yttria. This emission line might be due to Cr^{3+} in Al_2O_3. The crucibles, which are used during the firing of the sample, are made of Al_2O_3 contaminated with Cr^{3+}.

The reflection spectra of Fe^{3+}, Mn^{3+}, and Cr^{6+} (Figure 4) have one main similarity. They all exhibit a strong absorption around 254 nm. It is not possible to obtain a molar absorption coefficient from a reflection spectrum. However, using the Kubelka–Munk expression[31] (eq 1), the ratio between the molar absorption coefficient of the transition-metal ions and the Eu^{3+} ion at 254 nm can be derived from the reflection spectra. The Kubelka–Munk function ($F(R)$) is proportional to the molar absorption coefficient (ϵ). The Kubelka–Munk function can be written as follows:

$$F(R) = \frac{(1-R)^2}{2R} = \frac{K}{S} \propto \frac{\epsilon c}{S} \qquad (1)$$

where R is the reflection, K the absorption coefficient, S the scattering coefficient, and c the concentration of the codoped impurity.

Using eq 1, we can estimate from the reflection spectra that the molar absorption coefficient of the charge transfer band of Fe^{3+} at 254 nm is about 65 times larger than that of Eu^{3+} at the same wavelength. This large difference is noteworthy. The explanation has to be found in the fact that for the transition-metal ions the 3d orbital is involved in the charge-transfer transition, whereas for Eu^{3+} the shielded 4f orbital is involved in the charge-transfer transition. For Mn^{3+} the ratio between the molar absorption coefficients has the same order of magnitude. The CrO_4^{2-} ion has a 15 times larger molar absorption coefficient than Eu^{3+} at 254 nm.

These strong absorption bands of the transition-metal ions around 254 nm are competing with the Eu^{3+}–O^{2-} charge-transfer absorption for the mercury discharge radiation. Since these transition-metal ions have much larger molar absorption coefficients than Eu^{3+}, even a small amount of these transition-metal ions will absorb a large fraction of the exciting mercury discharge radiation. This competitive absorption leads to a decrease of the overall quantum yield (254-nm excitation) of $Y_{1.94}Eu_{0.06}O_3$:X (X (1000 ppm) is Fe, Mn, and Cr) samples (Table I).

The molar absorption coefficient of Fe^{3+} is larger than the molar absorption coefficient of CrO_4^{2-}. Therefore the decrease in quantum yield due to Fe^{3+} is expected to be larger than due to the same amount of CrO_4^{2-}. This is indeed the case. For Fe^{3+} and for CrO_4^{2-} energy transfer from Eu^{3+} to the impurity ions will not play an important role in the quantum yield decrease. Both impurities have no absorption at the energy resonant with the $^5D_0 \rightarrow {}^7F_J$ emission of Eu^{3+}.

The molar absorption coefficients of Mn^{3+} and of Fe^{3+} are approximately the same. Therefore the decrease of the quantum yield of $Y_{1.94}Eu_{0.06}O_3$:X due to competitive absorption induced by codoping with either 1000 ppm Fe^{3+} or 1000 ppm Mn^{3+} should be similar. However, codoping with Mn^{3+} results in a significantly larger decrease in quantum yield (254-nm excitation) than codoping with Fe^{3+}. The Mn^{3+} ion has an absorption band at the energy resonant with the Eu^{3+} emission. The larger decrease of the quantum yield is therefore ascribed to energy transfer from Eu^{3+} to Mn^{3+}.

The quantum yield reduction of $Y_{1.94}Eu_{0.06}O_3:Fe$ (254-nm excitation) is not a linear function of the Fe^{3+} concentration (Figure 6). In the region of high Fe^{3+} concentration the decrease of the quantum yield depends less strongly on the Fe^{3+} concentration than in the region of low Fe^{3+} concentration. The obtained curve is rather similar to the curve of the reflection versus the Fe^{3+} concentration. This curve shape has also been described by Fuller[9] for the quenching of the Eu^{3+} emission by Ce^{4+}. Fuller interpreted his results also by a competitive absorption mechanism.

(28) Huber, G.; Payne, S. A.; Chase, L. L.; Krupke, W. F. *J. Lumin.* **1988**, *39*, 259.
(29) McDaniel, M. P.; Martin, S. J. *J. Phys. Chem.* **1991**, *95*, 3289.
(30) Blasse, G. *Prog. Solid State Chem.* **1988**, *18*, 79.
(31) Kortüm, G. *Reflectance Spectroscopy, Principles, Methods, Applications*; Springer-Verlag: Berlin, 1969.

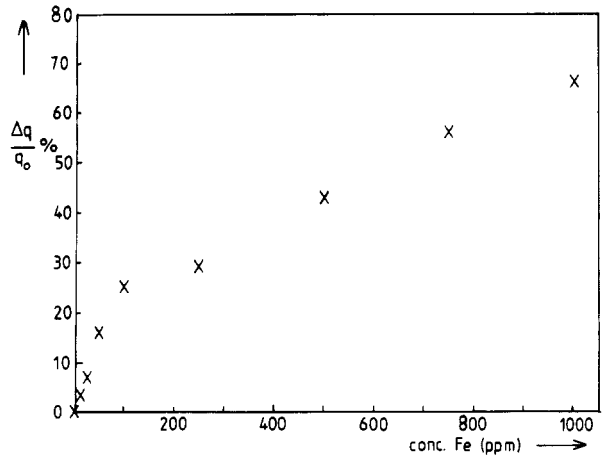

Figure 6. Dependence of the quantum yield reduction for 254-nm excitation ($q(Y_{1.94}Eu_{0.06}O_3) - q(Y_{1.94}Eu_{0.06}O_3{:}Fe^{3+}))/q(Y_{1.94}Eu_{0.06}O_3)$ on the Fe^{3+} concentration (Fe^{3+} concentration from 0 to 1000 ppm).

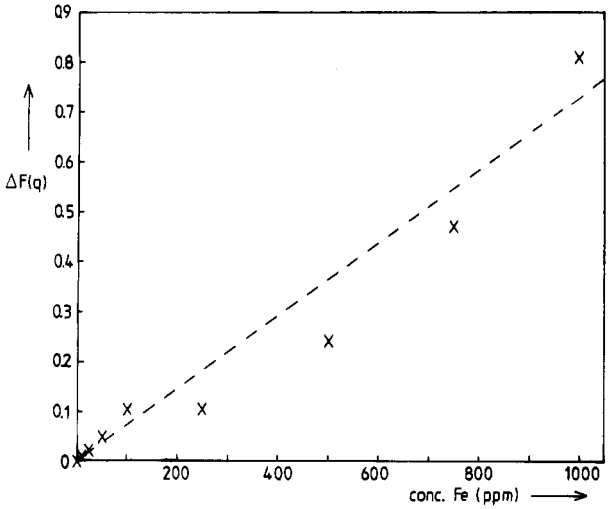

Figure 7. Dependence of the Kubelka–Munk function of the quantum yield for 254-nm excitation ($\Delta F(q)$) of $Y_{1.94}Eu_{0.06}O_3{:}Fe^{3+}$ on the Fe^{3+} concentration (Fe^{3+} concentration from 0 to 1000 ppm).

The dependence of the reflection at 280 nm of $Y_{1.94}Eu_{0.06}O_3$:Fe on the Fe^{3+} concentration is very well described by the Kubelka–Munk function (eq 1). The dependence of the quantum yield of $Y_{1.94}Eu_{0.06}O_3$:Fe (254-nm excitation) on the Fe^{3+} concentration has tentatively been fitted to the Kubelka–Munk function (Figure 7), since the decrease of the quantum yield is a result of an increase of the competitive absorption. To do so, we replace in eq 1 R by q.

Taking the relatively large uncertainty of the measured quantum yield into account, the correlation between the quantum yield and the Fe^{3+} concentration appears to be fairly well described by the Kubelka–Munk function. In practice this quantitative correlation can be used to give an estimate of the influence of a certain Fe^{3+} concentration on the quantum yield. It is estimated in this way, that the quantum yield of an optimized commercial $Y_{1.94}Eu_{0.06}O_3$ phosphor is decreased by about 7% by only 5 ppm of Fe^{3+} contamination.

Cerium and Terbium. The reflection spectrum of Y_2O_3:Tb (Figure 8) exhibits a very broad absorption band from 550 nm extending into the UV. There is no emission for excitation in this broad band. This absorption band is ascribed to the charge transfer transition of the tetravalent Tb^{4+} ion.[32] It is well-known that trivalent Tb^{3+} is

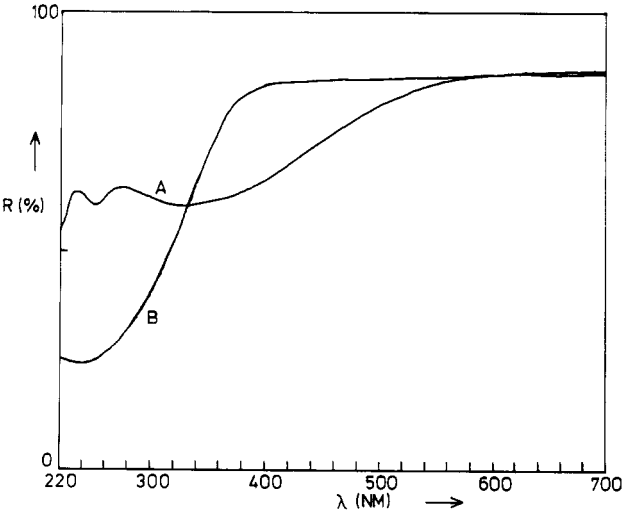

Figure 8. Reflection spectra of Y_2O_3:Tb (A) and Y_2O_3:Ce (B).

Table III. Relative Luminescence Quantum Yield of $Y_{1.94}Eu_{0.06}O_3$:X at 300 K for 254-nm Excitation (Coprecipitates)

$Y_{1.94}Eu_{0.06}O_3$:X (X: impurity)	quantum yield
blank fired in air	95
1000 ppm Tb	79
1000 ppm Ce	28

rather easily oxidized to the tetravalent state.[33] The extra net charge introduced by the tetravalent Tb^{4+} is probably compensated for by doubly ionized interstitial oxygens, as already discussed in the first part of this section. Upon excitation in the 4f–5d transition, at wavelengths shorter than 350 nm, the Tb^{3+} emission is found.[34]

The $Y_{1.94}Eu_{0.06}O_3$ samples codoped with 1000 ppm Tb show upon 254-nm excitation hardly any Tb^{3+} emission. This is not surprising, since the Eu^{3+} charge transfer and the 4f–5d transition of Tb^{3+} are excited in the same region of the spectrum. The excitation spectrum of the Tb^{3+} emission in $Y_{1.94}Eu_{0.06}O_3$:Tb does not show any transitions that could be ascribed to Eu^{3+}. This clearly shows the absence of energy transfer from the Eu^{3+} to Tb^{3+}. Trivalent Tb^{3+} has no 4f–4f transitions at the energy resonant with the $^5D_0 \rightarrow {}^7F_J$ emission of Eu^{3+}.

Nevertheless, the quantum yield (254-nm excitation) of $Y_{1.94}Eu_{0.06}O_3$:Tb (Table III) is lower than the quantum yield of a blank $Y_{1.94}Eu_{0.06}O_3$ sample which is prepared in the same way. Energy transfer from Eu^{3+} to tetravalent Tb^{4+} can also be excluded as a process responsible for decreasing the quantum yield, because the spectral overlap is small.

At 254 nm both Tb^{3+} and Tb^{4+} are able to compete with the Eu^{3+} ion for the excitation radiation. Using eq 1, it is estimated from the reflection spectra that the total molar absorption coefficient of $Tb^{3+/4+}$ (trivalent and tetravalent together) is about 5 times larger than that of Eu^{3+} at 254 nm. The contribution to the total absorption strength of trivalent and tetravalent $Tb^{3+/4+}$ cannot be separated. The absorption strength[35] of the 4f–5d transition of Tb^{3+} is expected to be of the same order of magnitude as the absorption strength of the charge transfer transition of Eu^{3+}. Since the concentration of Eu^{3+} is 30 times larger

(32) Hoefdraad, H. E. *J. Inorg. Nucl. Chem.* **1975**, *37*, 1917.
(33) Carnall, W. T. *Handbook on the Physics and Chemistry of Rare Earths*; Gschneidner, Jr., K. A., Eyring, L. J., Eds.; North Holland Publishing: Amsterdam, 1979; Chapter 24.
(34) Ropp, R. C. *J. Opt. Soc. Am.* **1967**, *57*, 213.
(35) Jørgensen, C. K. *Mol. Phys.* **1962**, *5*, 271.

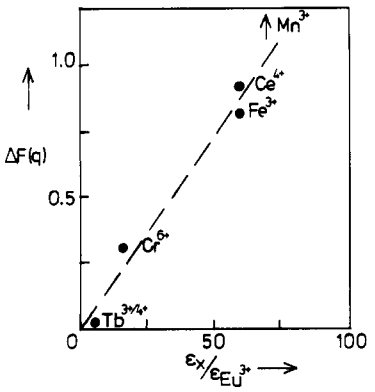

Figure 9. Dependence of the Kubelka–Munk function of the quantum yield for 254-nm excitation ($\Delta F(q)$) of $Y_{1.94}Eu_{0.06}O_3$:X (with X: Mn^{3+}, Ce^{4+}, Fe^{3+}, Cr^{6+}, $Tb^{3+/4+}$) on the molar absorption coefficients of the respective impurities (ϵ_X). The given molar absorption coefficients of the impurities are relative to the molar absorption coefficient of Eu^{3+} ($\epsilon_{Eu^{3+}}$) at 254 nm. The value for X = Mn^{3+} is off scale ($\Delta F(q) = 5$).

than the total $Tb^{3+/4+}$ concentration, the competitive absorption due to trivalent Tb^{3+} is not expected to have a large influence on the quantum yield. Therefore it is concluded that the decrease of the quantum yield is mainly caused by competitive absorption induced by tetravalent Tb^{4+}.

The reflection spectrum of $Y_{1.94}Eu_{0.06}O_3$:Ce is depicted in Figure 8. The very intense absorption band from 350 nm extending to shorter wavelengths is ascribed to tetravalent Ce^{4+}. Upon excitation in this absorption band no luminescence is observed. No separate absorption band due to trivalent Ce^{3+} could be observed. It is therefore likely that the Ce^{3+} ion is oxidized to the tetravalent state. The Ce^{3+} ion is even more easily oxidized than the Tb^{3+} ion.[33]

Energy transfer and reabsorption can be ruled out as processes which could be responsible for the observed low quantum yield (254-nm excitation) of $Y_{1.94}Eu_{0.06}O_3$ codoped with 1000 ppm Ce (Table III). The decrease is a result of competitive absorption by the tetravalent state of Ce^{4+}.

Using eq 1, it is estimated from the reflection spectra that the molar absorption coefficient of Ce^{4+} is about 65 times larger than the molar absorption coefficient of Eu^{3+} at 254 nm. This is a similar ratio as is reported for Ce^{4+} and Eu^{3+} in nitrile solution.[36] It should be expected that the decrease of the quantum yield as a result of codoping with Ce^{4+} is of the same order of magnitude as when codoped with the same amount of Fe^{3+}, since they have similar molar absorption coefficients at 254 nm. This is indeed the case.

In the previous section the decrease of the quantum yield was described by the Kubelka–Munk function ($\Delta F(q)$). According to eq 1 the Kubelka–Munk function should be linear not only with the concentration of the impurity but also with the molar absorption coefficient. In Figure 9 this is tentatively depicted. The ratio of the molar absorption coefficients of the impurities and of Eu^{3+} (at 254 nm) seems a rather accurate measure to estimate the quantum yield reduction due to codoping with 1000 ppm impurity. Only Mn^{3+} is not in line with this reasoning, but in the case of Mn^{3+} energy transfer from Eu^{3+} to Mn^{3+} plays also a role in decreasing the quantum yield.

Conclusions

The decrease of the quantum yield for 254-nm excitation of $Y_{1.94}Eu_{0.06}O_3$ as a result of codoping with impurities is successfully described with a competitive absorption model. The absorption strength of the impurity at 254 nm determines the decrease of the quantum yield. Impurities with very large molar absorption coefficients at 254 nm are Ce^{4+}, Fe^{3+}, and Mn^{3+}. The presence of these ions as impurities results in a large decrease of the quantum yield of $Y_{1.94}Eu_{0.06}O_3$ for excitation at 254 nm. The presence of Mn^{3+} results in an additional decrease of the quantum yield due to the Eu^{3+}–Mn^{3+} energy transfer. The dependence of the quantum yield on the Fe^{3+} concentration can be described by the Kubelka–Munk correlation.

The presence of interstitial oxygen leads to absorption in the UV. This competitive absorption leads to a reduction of the quantum yield for 254-nm excitation of $Y_{1.94}Eu_{0.06}O_3$. For 185-nm excitation the energy transfer to interstitial oxygen competes with energy transfer to the Eu^{3+} ions. Thus the interstitial oxygens also lead to a decrease of the quantum yield for 185-nm excitation.

The tetravalent state of Tb^{4+} and especially of Ce^{4+} leads to strong competitive absorption and hence to a decrease of the quantum yield (254-nm excitation).

Acknowledgment. This research is part of the EURAM-BRITE RELUM project (BREU-147). We thank the European Community for financial support of these investigations. We are grateful to Mr. J. J. Braconnier (Rhône-Poulenc) for supplying the starting materials and to Mr. C. Bakker (Philips Lighting B.V.) for performing the quantum yield measurements.

Registry No. $Y_{1.94}Eu_{0.06}O_3$, 109657-75-2; Zr^{4+}, 15543-40-5; Ca^{2+}, 14127-61-8; Tb, 7440-27-9; Cl, 7440-45-1; Fe, 7439-89-6; Mn, 7439-96-5; Cr, 7440-47-3; O_2, 7782-44-7.

(36) Ryan, J. L.; Jørgensen, C. K. *J. Phys. Chem.* **1966**, *70*, 2845.